The EMBO Journal (2005), 1–14 | © 2005 European Molecular Biology Organization | All Rights Reserved 0261-4189/05
www.embojournal.org

THE EMBO JOURNAL

The eIF1A C-terminal domain promotes initiation complex assembly, scanning and AUG selection *in vivo*

Christie A Fekete[1], Drew J Applefield[2], Stephen A Blakely[1], Nikolay Shirokikh[3], Tatyana Pestova[3], Jon R Lorsch[2] and Alan G Hinnebusch[1,*]

[1]Laboratory of Gene Regulation and Development, National Institute of Child Health and Human Development, NIH, Bethesda, MD, USA, [2]Department of Biophysics and Biophysical Chemistry, Johns Hopkins University School of Medicine, Baltimore, MD, USA and [3]Department of Microbiology and Immunology, State University of New York Health Science Center at Brooklyn, Brooklyn, NY, USA

Translation initiation factor 1A stimulates 40S-binding of the eukaryotic initiation factor 2 (eIF2)/GTP/Met-tRNA$_i^{Met}$ ternary complex (TC) and promotes scanning *in vitro*. eIF1A contains an OB-fold present in bacterial IF1 plus N- and C-terminal extensions. Truncating the C-terminus (Δ*C*) or mutating OB-fold residues (*66–70*) of eIF1A reduced general translation *in vivo* but increased *GCN4* translation (Gcd$^-$ phenotype) in a manner suppressed by overexpressing TC. Consistent with this, both mutations diminished 40S-bound TC, eIF5 and eIF3 *in vivo*, and Δ*C* impaired TC recruitment *in vitro*. The assembly defects of the OB-fold mutation can be attributed to reduced 40S-binding of eIF1A, whereas Δ*C* impairs eIF1A function on the ribosome. A substitution in the C-terminal helix (*98–101*) also reduced 43S assembly *in vivo*. Rather than producing a Gcd$^-$ phenotype, however, *98–101* impairs *GCN4* derepression in a manner consistent with defective scanning by reinitiating ribosomes. Indeed, *98–101* allows formation of aberrant 48S complexes *in vitro* and increases utilization of non-AUG codons *in vivo*. Thus, the OB-fold is crucial for ribosome-binding and the C-terminal domain of eIF1A has eukaryotic-specific functions in TC recruitment and scanning.

The EMBO Journal advance online publication, 29 September 2005; doi:10.1038/sj.emboj.7600821
Subject Categories: proteins
Keywords: eIF1A; eIF2; GCN4; scanning; translation

Introduction

Translation initiation begins with the binding of Met-tRNA$_i^{Met}$ to the 40S ribosomal subunit in a ternary complex (TC) with eukaryotic initiation factor 2 (eIF2) and GTP. This reaction is stimulated *in vitro* by eIF1, eIF1A and eIF3 (Hinnebusch, 2000; Algire *et al*, 2002; Majumdar *et al*, 2003; Kolupaeva *et al*, 2005). The 43S preinitiation complex (PIC) thus formed binds to the 5′-end of mRNA and scans the leader until Met-tRNA$_i^{Met}$ base-pairs with an AUG, triggering GTP hydrolysis by eIF2 in a reaction stimulated by eIF5 (Hershey and Merrick, 2000). Biochemical evidence indicates that mammalian eIF1 and eIF1A promote scanning and formation of a 48S complex at the start codon (Pestova *et al*, 1998). eIF2, eIF5, eIF1 and eIF3 have been implicated in AUG selection, as mutations in these factors permit increased initiation at a UUG codon in yeast (Donahue, 2000; He *et al*, 2003; Valasek *et al*, 2004). Consistent with this, eIF1 inhibits 48S assembly at near-cognate triplets or AUGs in a poor context *in vitro* (Pestova and Kolupaeva, 2002).

While biochemical studies have implicated eIF3, eIF1 and eIF1A in 40S-binding of TC, their relative importance *in vivo* and functions in 43S assembly are poorly understood. The TC in yeast cells is linked to eIF3, eIF5 and eIF1 in a multifactor complex (MFC) (Asano *et al*, 2000), and evidence is accumulating that these interactions promote cooperative binding of MFC components to the 40S ribosome *in vivo* (Asano *et al*, 2001; Valášek *et al*, 2002, 2003; Nielsen *et al*, 2004; Singh *et al*, 2004). We presented genetic evidence that eIF1A is required for wild-type (WT) binding of TC to 40S subunits in yeast, as deleting the C-terminal domain and adjacent 3_{10} helix of eIF1A (the Δ*108–153* mutation) increased translation of *GCN4* mRNA in cells lacking protein kinase GCN2 (Olsen *et al*, 2003). *GCN4* translation is normally induced in amino-acid-starved cells by phosphorylation of eIF2 (Hinnebusch, 1996). The ensuing reduction in TC concentration allows 40S subunits that translate the first upstream open-reading frame (uORF1) and resume scanning to bypass the three remaining uORFs and reinitiate downstream at *GCN4*. In nonstarved WT or *gcn2*Δ cells, by contrast, a high level of TC ensures that all 40S subunits scanning downstream from uORF1 quickly rebind TC, reinitiate at uORFs 2, 3 or 4 and dissociate from the mRNA without translating *GCN4* (Hinnebusch, 1996). Importantly, the derepressed *GCN4* translation in *gcn2*Δ cells (Gcd$^-$ phenotype) produced by the Δ*108–153* mutation was suppressed by overexpressing the TC. This suggested that the rate of TC binding to 40S subunits scanning downstream from uORF1 was reduced by Δ*108–153*, allowing a fraction to bypass uORFs 2–4 and reinitiate at *GCN4* instead (Olsen *et al*, 2003). However, this interpretation was not confirmed biochemically; nor was it determined whether Δ*108–153* impairs 40S-binding of eIF1A or disrupts its biochemical function in 43S assembly.

eIF1A is related to bacterial IF1, and both proteins contain the β-barrel 'OB'-fold (Sette *et al*, 1997; Battiste *et al*, 2000), while eIF1A also contains an α-helical domain and random-coil N- and C-terminal extensions (NTD and CTD) (Figure 1A). As IF1 binds to the A-site of the 30S subunit

*Corresponding author. Laboratory of Gene Regulation and Development, National Institute of Child Health and Human Development, NIH, Building 6A/Room B1A-13, Bethesda, MD 20892, USA. Tel.: +1 301 496 4480; Fax: +1 301 496 6828;
E-mail: ahinnebusch@nih.gov

Received: 2 June 2005; accepted: 26 August 2005

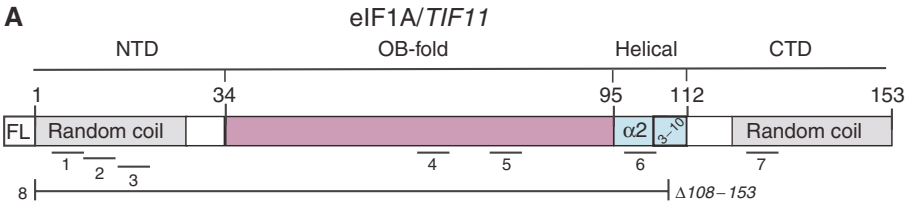

B

	FL-TIF11 allele	Growth 30°C	Growth 37°C	Growth 3-AT	Expression
	WT	+++++	+++++	–	
	GKKNT$_{2-6}$AAAAA	+++	+++	–	
1	*KGGKK$_{7-11}$AAAAA*	lethal	lethal	N/A	
2	*GRRGK$_{12-16}$AAAAA*	lethal	lethal	N/A	
NTD 3	*NDSDG$_{17-21}$AAAAA*	++	++	–	
	PKRELIY$_{22-28}$AAAAAAA	+++	++	–	
	KEEGQE$_{29-34}$AAAAQA	+++	++	–	
	MLGN$_{41-44}$ALAA	++++	+++	–	
	GRVE$_{45-48}$AAVA	++	++	–	
4	hc *DGNK$_{53-56}$AANA*	++	+	+	*
OB	*R62D*	lethal	lethal	N/A	
5	*RKKVW$_{66-70}$AAAVA*	++	++	++	
	hc *RDFQD$_{82-86}$AAAAA*	+	+	–	*
	KYN$_{94-96}$AYA	+++	+	–	
6	*DEAR$_{98-101}$AAAA*	+++	+++	–	
Helical	*KN$_{104-105}$AA*	+++++	+++++	–	
	PE$_{110-111}$AA	+++++	++++	–	
	NE$_{116-117}$AA	lethal	lethal	N/A	
	TDNFG$_{118-122}$AAAAA	+++++	+++++	–	
	FESDE$_{123-127}$AAAAA	+++++	+++++	–	
	DVNFE$_{128-132}$AAAAA	++++	+++	++	
7	*F131A, F133A*	+	+	+	
CTD	*FGNAD$_{133-137}$AAAAA*	++++	+++	++	ND
	EDDEE$_{138-142}$AAAAA	+++	+++	–	
	GEDEEL$_{143-148}$AAAAAA	+++	+++	–	
	DIDDI$_{149-153}$AAAAA	+++	++	–	
8	hc *Δ108–153*	+++	+	++++	*

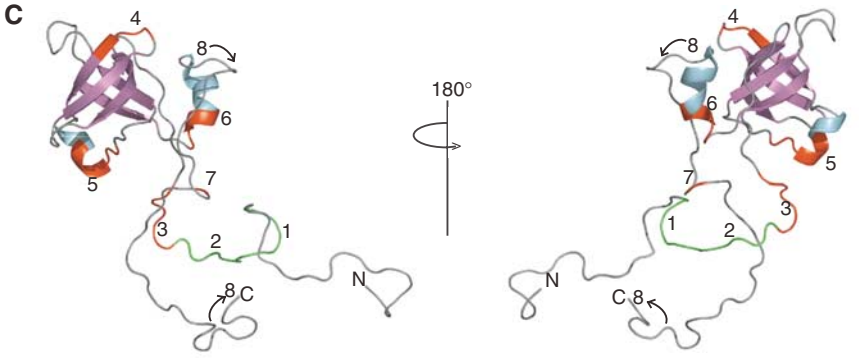

Figure 1 Phenotypes of eIF1A mutations. (**A**) Schematic representation of eIF1A domain organization, including the FLAG (FL) epitope, amino-acid positions (above) and locations of key mutations (1–8; underlined below). (**B**) Growth of *gcn2*Δ strains harboring the indicated mutant or WT *FL-TIF11* alleles on SC medium lacking Leu (SC-L) at 30 or 37°C and on SC medium lacking leucine and histidine (SC–LH) and containing 10 mM 3-AT at 30°C. Relative growth is summarized on a scale from (–) to (+ + + + +). The domain locations of the mutations are listed on the left along with designations of selected mutations 1–8 as indicated in panel A. The far-right column (Expression) contains results of Western analysis of WCEs from the same strains analyzed for growth phenotypes (except for the lethal alleles) using FLAG antibodies. Separate probing of the blots with antibodies against eIF2α ensured similar protein loading for each extract (not shown). Three *FL-TIF11* alleles (*) were expressed on hc plasmids; ND, not detectable. Four additional lethal alleles were identified for which no protein products were detected: *K64A*, *K67D*, *Q85A* and *HIRGK$_{60-64}$AAAA* (data not shown). (**C**) Predicted locations of residues altered by mutations 1–8 (described in panel A) in the 3D structure of eIF1A, designated red (viable alleles) or green (lethal alleles), as determined using MacPyMOL (DeLano, 2002).

(Moazed *et al*, 1995; Carter *et al*, 2001), the OB-fold in eIF1A most likely binds to the A-site of 40S subunits in eukaryotes. To assign its functions to specific residues, we mutated conserved surface-exposed residues in the OB-fold, α-helical domains, NTD and CTD of yeast eIF1A, reasoning that such residues would mediate eIF1A interactions with the ribosome or other eIFs. From genetic and biochemical analysis of substitutions in the OB-fold and helical domain, and of the Δ*108–153* mutation described previously, we conclude that the OB-fold plays a key role in ribosome-binding while the helical domain and CTD function in 43S assembly and scanning.

Results

Mutagenesis of conserved surface residues of yeast eIF1A

Using the 3D structure of human eIF1A (Battiste *et al*, 2000) and sequence alignments of eIF1A from different species, we constructed mutations of conserved surface-exposed residues in the OB-fold and α-helical domains of yeast eIF1A (Figure 1), in most cases substituting three to five contiguous residues with alanines. We also made consecutive blocks of Ala substitutions in the NTD and CTD. All mutations were generated in an *FL-TIF11* allele on a single-copy plasmid, bearing the *TIF11* promoter and coding sequences for FLAG (FL) epitope at the 5′-end of the ORF (Olsen *et al*, 2003). The mutant alleles were used to replace episomal WT *TIF11* (*TIF11*$^+$) in a *tif11*Δ *gcn2*Δ strain by plasmid-shuffling.

Eight of the clustered substitutions were lethal (Figure 1B and legend), preventing eviction of *TIF11*$^+$ from the strain. Western analysis of whole-cell extracts (WCEs) from strains harboring both *FL*-tagged mutant alleles and untagged *TIF11*$^+$ with FL antibodies showed that four of the lethal alleles (altering residues 60–64, 67 or 85) produced no detectable protein and were not studied further. The other four lethal alleles produced WT levels of protein (Figure 1B), implying that they disrupt an essential function of eIF1A. We compared the 40S-binding of WT and two of the FL-tagged mutants containing the lethal substitutions *R62D* or *NE*$_{116–117}$*AA* in cells expressing untagged eIF1A using a chemical crosslinking assay described below. The OB-fold mutation *R62D* strongly reduced 40S-binding of eIF1A to only ∼17% of WT, whereas the CTD mutation *NE*$_{116–117}$*AA* impaired 40S-binding by <30% (data not shown). A nonlethal OB-fold mutation discussed below decreased 40S-binding more so than did *NE*$_{116–117}$*AA*, suggesting that the latter probably disrupts an essential function of eIF1A carried out on the ribosome.

Western analysis of the 22 nonlethal *tif11* mutants after eviction of *TIF11*$^+$ showed that all but three produced WT levels of eIF1A (Figure 1B). The three exceptional alleles, *DGNK*$_{53–56}$*AANA*, *RDFQD*$_{82–86}$*AAAAA* and Δ*108–153*, required overexpression to compensate for reduced steady-state levels, and when present on high-copy (hc) plasmids, produced protein levels ∼3-fold higher than WT. All subsequent analysis was conducted with the hc versions of these alleles.

The viable mutants containing only *FL*-tagged alleles were compared to the *FL-TIF11*$^+$ strain for growth on complete medium (SC) and on SC lacking histidine and containing 3-aminotriazole (3-AT), an inhibitor of histidine biosynthesis. The *gcn2*Δ mutation in these strains blocks induction of *GCN4* translation and attendant derepression of histidine biosynthetic enzymes regulated by GCN4. Mutations that derepress *GCN4* translation independently of eIF2 phosphorylation suppress the 3-AT-sensitive phenotype (3-AT^S) of *gcn2*Δ cells, producing a Gcd$^-$ phenotype. All but three of the 21 nonlethal substitutions produced a slow-growth phenotype (Slg$^-$) on SC, and five of these conferred 3-AT-resistance (3-AT^R) (Figure 1B). The Δ*108–153* deletion produced both Slg$^-$ and 3-AT^R phenotypes, as reported previously (Olsen *et al*, 2003).

The RKKVW$_{66–70}$*AAAVA and Δ108–153 mutations disrupt PIC assembly by different mechanisms*

Among the new Gcd$^-$ alleles, *RKKVW*$_{66–70}$*AAAVA* was of interest because it restored growth on 3-AT medium while strongly impairing growth on SC (Figure 2B). Indeed, *RKKVW*$_{66–70}$*AAAVA* elicits greater depletion of polysomes and accumulation of 80S monosomes than does Δ*108–153* (Figure 2A), indicating a strong defect in translation initiation. (Henceforth, we abbreviate *RKKVW*$_{66–70}$*AAAVA* and Δ*108–153* as *66–70* and Δ*C*, respectively.) Importantly, the 3-AT^R/Gcd$^-$ phenotype of *66–70* was suppressed by overexpressing all three eIF2 subunits and tRNA$_i^{Met}$ from an hc plasmid (hc-TC) (Figure 2B, cf. rows 4–5), as observed for Δ*C* (Olsen *et al*, 2003) (cf. rows 6–7). Hence, both *66–70* and Δ*C* appear to derepress *GCN4* by reducing TC binding to scanning 40S ribosomes. Note that overexpressing TC also reduces the derepression of *GCN4* that occurs when TC recruitment is impaired by eIF2 phosphorylation in starved *GCN2*$^+$ cells (Dever *et al*, 1995). We quantified the Gcd$^-$ phenotype of the *66–70* mutant by assaying a *GCN4-lacZ* reporter containing all four uORFs, which is normally expressed at low levels in *gcn2*Δ cells owing to the absence of eIF2α phosphorylation. The *66–70* strain showed ∼5-fold greater *GCN4-lacZ* expression than did the *TIF11*$^+$*gcn2*Δ strain (Figure 2C), whereas Δ*C* produced ∼8-fold derepression of *GCN4-lacZ* expression, in accordance with previous results (Olsen *et al*, 2003). Derepression of *GCN4-lacZ* in a *GCN2 TIF11* strain treated with 3-AT was considerably higher (15-fold; data not shown), indicating that these mutations only partially suppress reinitiation at uORFs 2–4. As discussed below, this probably occurs because eIF1A mutations produce multiple initiation defects with offsetting effects on *GCN4* translation.

The 3-AT^R phenotypes of the other four Gcd$^-$ mutations described in Figure 1 were not suppressed by hc-TC (data not shown). Presumably, these mutations allow a fraction of the 40S subunits that have rebound TC to leaky-scan past uORF4 and reinitiate at *GCN4*. This class of mutations was not analyzed further.

To obtain biochemical support for our interpretation of the genetic results on the *66–70* and Δ*C* mutants, we measured binding of eIF2 to 40S PICs in WCEs of cells treated with formaldehyde. This treatment crosslinks factors to 40S ribosomes *in vivo*, minimizing dissociation of PICs during sedimentation through sucrose gradients without addition of heparin as a stabilizing agent (Nielsen *et al*, 2004). The crosslinks are reversed by heating prior to resolving the fractions by SDS–PAGE for Western analysis. Typical results of this assay are shown in Figure 2D and the results of replicate experiments are quantified in Figure 2E. (Henceforth, we use the term 40S-binding to describe the

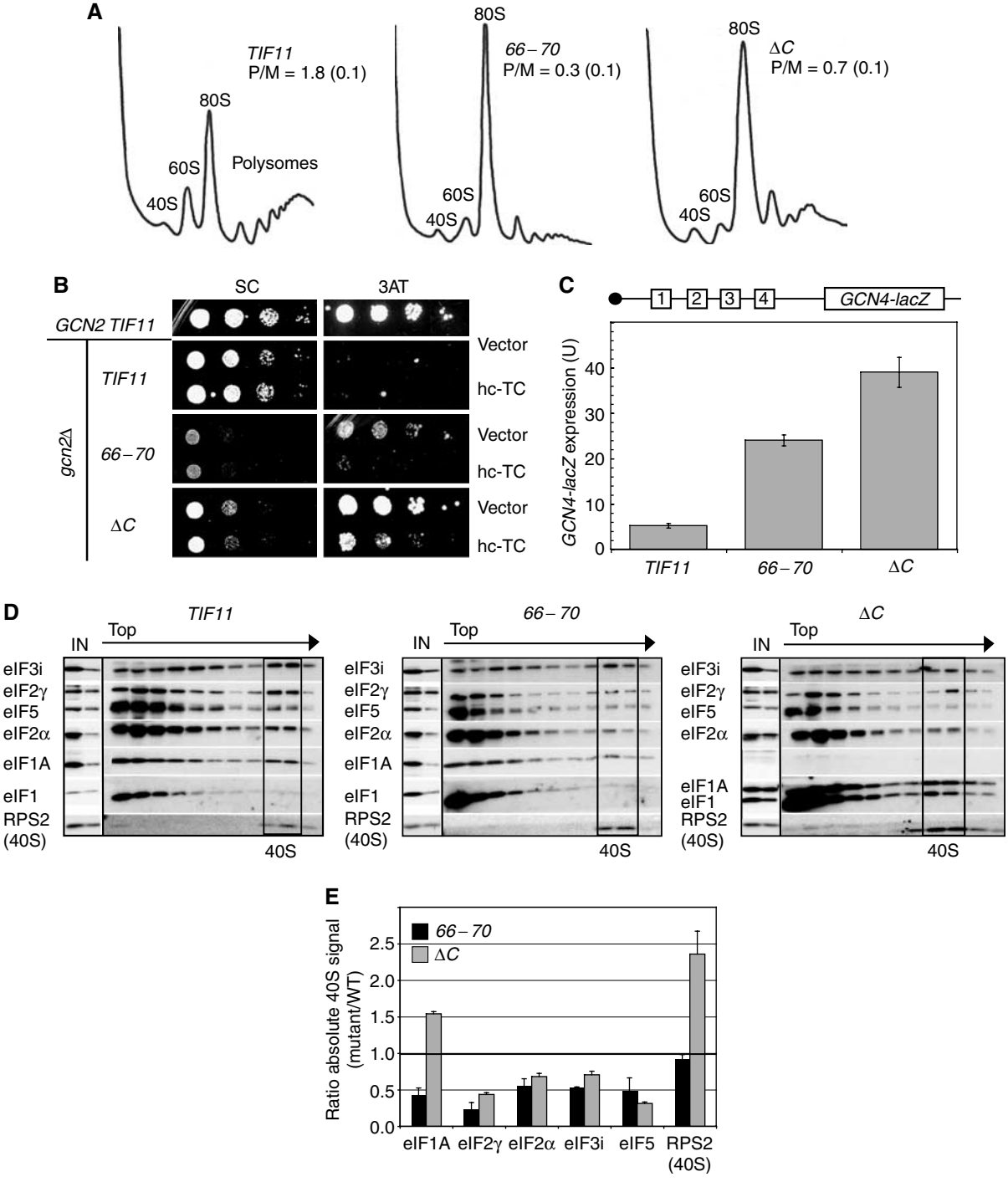

Figure 2 The *66–70* and Δ*C* mutations produce general reductions in translation initiation, derepressed translation of *GCN4* and decreased 43S complex formation *in vivo*. (**A**) Polysome profiles of *gcn2*Δ strains harboring WT (H2999), *66–70* (H3580) or Δ*C* (H3002) alleles of *TIF11-FL* after culturing in SC-L medium to $OD_{600} \approx 1$ and crosslinking cells with 1% (v/v) HCHO. WCEs were resolved by sedimentation through 4.5–45% sucrose gradients and gradients were scanned at A_{254}. The polysome/monosome ratios (P/M, means ± s.e., $n = 3$) are indicated for each strain. (**B**) Slg^- and Gcd^- phenotypes were assayed by spotting serial 10-fold dilutions of the *gcn2*Δ strains described in (A) and isogenic *GCN2 TIF11* strain H1642 (harboring YCplac111), on SC-L or SC-LH + 10 mM 3-AT at 30°C. (**C**) Expression of the chromosomal *GCN4-lacZ* reporter depicted schematically was measured in the strains described in (A) grown in SC-L medium. β-Galactosidase activity in units (U) of nmol ONPG cleaved/min/mg was measured in WCEs from three three independent transformants and the mean and s.e. ($n = 6$) values were plotted in the histogram. (**D**) 43S assembly was measured in the strains described in (A) after crosslinking cells with HCHO, as described in (A). WCEs were resolved by sedimentation through 7.5–30% sucrose gradients and gradient fractions were subjected to Western analysis using the indicated antibodies. In all, 1 and 0.2% aliquots of each input WCE (IN) were analyzed in parallel. The fractions containing free 40S subunits are boxed. (**E**) Initiation factor binding to 40S subunits in the experiment shown in (D), and in two replicate experiments, was quantified by calculating the ratio of the 40S signal in the mutant relative to the WT. The results are means ± s.e. ($n = 3$). The line at $y = 1.0$ indicates the WT level of binding.

association of factors with either free 40S subunits or 43S/48S PICs, which cannot be distinguished in this assay.)

The 40S-binding of the *66–70* mutant protein was reduced to <50% of WT, whereas the Δ*C* protein bound at a greater than WT level, probably reflecting its overexpression (Figures 2D and E). Interestingly, *66–70* also reduced the 40S-binding of the TC components eIF2α and eIF2γ, eIF3 and eIF5 to ⩽50% of WT. Similar results were obtained for the Δ*C* mutant (Figures 2D and E). (We chose not to quantify the 40S-binding of eIF1 in these experiments because it is overexpressed in the mutants and it frequently does not show an obvious peak in the 40S fractions of WT cells.) The total amounts of eIF3i, eIF2γ and eIF5 over the entire gradient were somewhat lower in the *66–70* and Δ*C* mutants versus WT (Figure 2D), even though these factors were present at WT levels in the WCEs applied to the gradients (cf. 'IN' lanes). Hence, it appears that the unbound factors are more susceptible to degradation during centrifugation in the mutant extracts. This phenomenon was described previously for mutations in the c/NIP1 subunit of eIF3 (Valasek *et al*, 2004). Despite the reductions in total levels of eIF3i, eIF2γ and eIF5 in the gradients, their distributions were altered such that the proportions in the 40S fractions were reduced with corresponding increases in fractions closer to the top of the gradient (Supplementary Figures S1 and S2). Thus, it appears that eIF1A is required for optimal 40S-binding of TC, eIF3 and eIF5, and that both *66–70* and Δ*C* impair these assembly reactions *in vivo*.

In accordance with the fact that hc-TC suppressed the Gcd$^-$ phenotypes of *66–70* and Δ*C*, hc-TC restored 40S-binding of eIF2α and eIF2γ to WT or higher levels in both mutants, and eIF3i binding in the *66–70* strain (cf. Figures 3A and B; quantification in Figure 3C). By contrast, hc-TC did not rescue 40S-binding of eIF5 in either mutant (Figure 3C). The large amounts of eIF2 subunits in the extracts containing hc-TC made it somewhat difficult to discern 40S-binding of eIF2 from trailing of eIF2 from the upper fractions into the 40S fractions. To confirm our conclusions, we resedimented the 40S fractions from gradients similar to those shown in Figures 3A and B and quantified the factors that cosedimented a second time with the 40S subunits. The results in Figure 3D confirm that *66–70* and Δ*C* impair 40S-binding of eIF2, eIF3 and eIF5, and also that hc-TC restores 40S-binding of eIF2, but not eIF5, by mass action. Hence, eIF1A promotes eIF5 recruitment independent of its effect on TC, and it enhances eIF3 recruitment by mechanisms both TC-dependent (evident in *66–70* cells) and TC-independent (evident in Δ*C* cells).

The fact that hc-TC did not restore WT 40S-binding of eIF5 in both mutants fits with our finding that the Slg$^-$ phenotypes of these mutants were not suppressed by hc-TC (Figure 2B), indicating a rate-limiting defect distinct from TC recruitment. Consistent with this, overexpressing eIF5 partially suppressed the Slg$^-$ phenotype of *66–70* (Figure 3E) and increased 40S-binding of eIF5, but did not alter 40S-binding of other factors or of the mutant eIF1A itself (Supplementary Figure S3). Thus, reduced 40S-binding of eIF5 is partly responsible for the strong initiation defect in *66–70* cells. Overexpressing eIF5 did not reduce the Slg$^-$ phenotype of the Δ*C* mutant, indicating an additional rate-limiting defect in this strain. As shown below, Δ*C* impairs ribosomal scanning and AUG recognition.

The 40S-binding of eIF1A was reduced by *66–70* to ∼50% of the WT level (Figures 2D and E). From the crystal structure of the IF1–30S complex (Carter *et al*, 2001), it can be predicted that this mutation substitutes OB-fold residues that interact with the A-site of the 40S subunit. Hence, the defects conferred by *66–70* could result from diminished ribosome binding of the mutant eIF1A. Supporting this idea, introducing *66–70* on an hc plasmid partly suppressed its Slg$^-$ and 3-AT^R/Gcd$^-$ phenotypes (Figure 4A) and produced a greater than WT level of 40S-binding by the mutant eIF1A protein (Figures 4B and C) Thus, the 40S-binding defect of the *66–70* protein can be corrected by mass action. The hc *66–70* allele also increased 40S-binding of eIF2, eIF3 and eIF5 compared to that seen with sc *66–70*, albeit not to WT levels (Figures 4B and C). The residual 43S assembly defects and Slg$^-$ phenotype (Figure 4A) in cells with hc *66–70* suggest that eIF1A function in PIC assembly is impaired by this mutation apart from its effects on 40S-binding of eIF1A itself.

To determine whether *66–70* impairs direct contact between eIF1A and the 40S subunit, we analyzed its effect on binding of fluorescently tagged eIF1A to purified 40S ribosomes. Tetramethylrhodamine (TAMRA)-labeled WT eIF1A was prebound to 40S subunits and unlabeled mutant or WT eIF1A was added to compete for binding of labeled eIF1A. The decrease in fluorescence anisotropy as a function of the concentration of mutant proteins allowed us to calculate the K_d for each mutant (Maag and Lorsch, 2003). As shown in Figures 4D and E, the *66–70* mutant has a K_d ∼90-fold greater than that of WT eIF1A, whereas the Δ*C* mutant binds to 40S subunits with WT or higher affinity. These data indicate that *66–70*, but not Δ*C*, reduces the intrinsic affinity of eIF1A for the 40S ribosome.

We also asked whether the Δ*C* and *66–70* mutations impair the rate of PIC assembly *in vitro*. Preformed TC containing [^{35}S]-Met-tRNA$_i^{Met}$ was incubated with 40S subunits, eIF1, a model mRNA, and either mutant or WT eIF1A, and the fraction of labeled [^{35}S]-Met-tRNA$_i^{Met}$ bound to 40S subunits was measured with a native gel assay (Algire *et al*, 2002). As shown in Figure 4F, Δ*C* greatly reduced the rate of TC binding to 40S subunits in this assay. The Δ*C* mutant retains some activity, as the rate of TC binding was ⩾2-fold higher than in the absence of eIF1A and reached the same end point given by WT protein after 20 min (data not shown). The *66–70* protein also showed a strong defect in TC binding; however, this defect was suppressed when using a concentration of *66–70* protein large enough to overcome its 40S-binding defect (10 μM) (Figure 4F). These findings support the idea that Δ*C* decreases the ability of 40S-bound eIF1A to stimulate TC recruitment, whereas *66–70* primarily impairs 40S-association of the mutant protein.

TC overexpression suppresses the Slg$^-$ and 43S assembly defects in the helical domain DEAR$_{98–101}$AAAA mutant

Unlike the *66–70* and Δ*C* mutations, the *DEAR$_{98–101}$AAAA* substitution in the helical domain (Figure 1C, #6; abbreviated below as *98–101*) produced a Slg$^-$ phenotype that is partially suppressed by hc TC (Figure 5A). Consistent with this, hc-TC decreased polysome runoff and accumulation of 80S monosomes in this mutant (Figure 5C; cf. last two profiles). *In vivo* analysis of 43S complexes revealed >50% reductions in

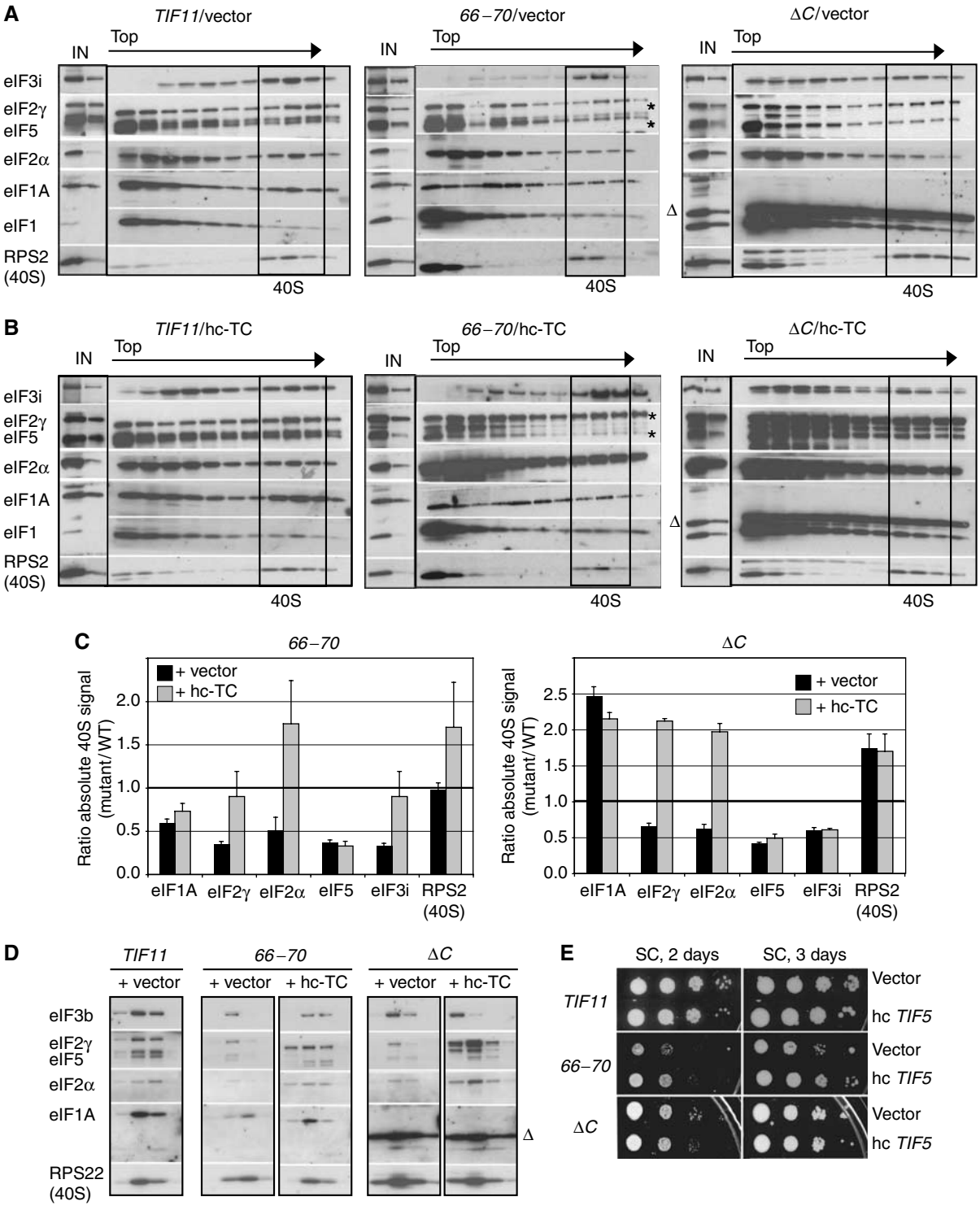

Figure 3 Overexpression of TC restores WT binding of TC, but not eIF5, in the *66–70* and Δ*C* mutants. (**A, B**) 43S assembly was measured in HCHO crosslinked cells of the *gcn2*Δ strains described in Figure 2A transformed with empty vector YEp24 (A) or p1780-IMT (hc-TC) (B), exactly as described in Figure 2. 'Δ' indicates the Δ*C* product; '*' indicate that darker exposures of the indicated panels were presented. (**C**) The results in (A) and (B) were quantified as in Figure 2E, showing the means ± s.e. from three experiments. (**D**) 40S fractions from gradients similar to (A) and (B) were subjected to resedimentation through a second sucrose gradient. Western analysis of gradient fractions containing 40S peaks in each strain is shown. (**E**) Overexpression of eIF5 (*TIF5*) partially suppresses the Slg$^-$ phenotype of the *66–70* mutant. Serial 10-fold dilutions of the *gcn2*Δ strains from Figure 2A transformed with empty vector YEp24 or hc *TIF5* plasmid YEpTIF5-U were spotted on SC-U and grown at 30°C as indicated.

40S-bound eIF2 subunits and also reductions in 40S-binding of eIF3 (by ~40%), eIF5 (by 80%) and eIF1A itself (by 55%), suggesting that *98–101* causes a broad defect in 43S assembly (Figures 6A and B, cf. *TIF11*/vector and *98–101*/vector, and 6C). (As described above, there were reduced levels of eIF2, eIF3 and eIF1A in fractions at the top of the gradient, but these reductions were not evident in the input WCEs, suggesting that they arise from degradation of unbound factors in

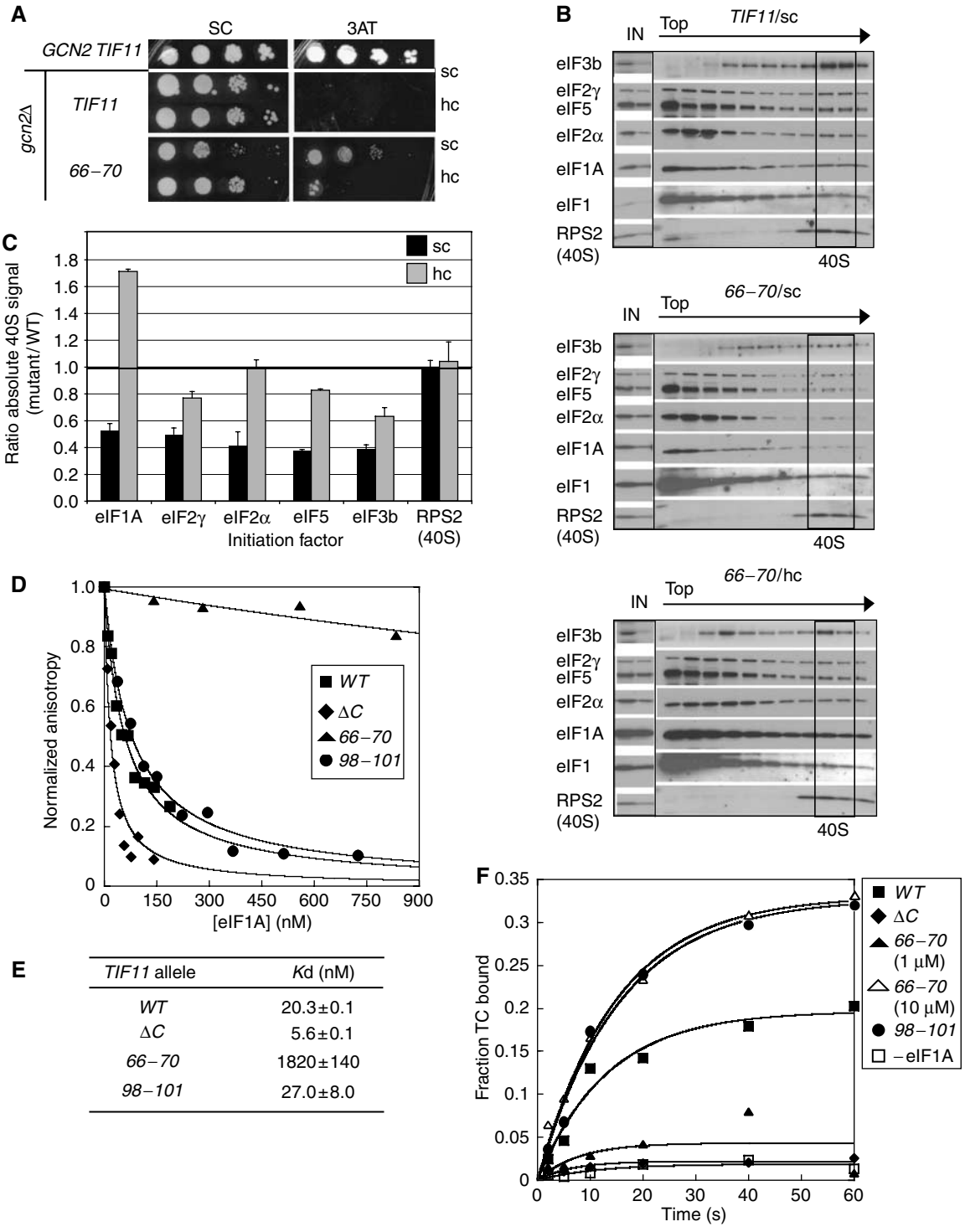

TIF11 allele	*K*d (nM)
WT	20.3±0.1
Δ*C*	5.6±0.1
66–70	1820±140
98–101	27.0±8.0

Figure 4 Overexpressing the *66–70* mutant diminishes its Slg$^-$ and Gcd$^-$ phenotypes, and the mutant is defective for 40S-binding *in vitro*. (**A**) Serial dilutions of *gcn2*Δ strains carrying the WT (H2999) or *66–70-tif11-FL* alleles on sc or hc plasmids (strains H3580 and H3581, respectively), and H1642 transformed with YCplac111, were spotted on SC-L and SC-LH + 10 mM 3-AT and grown at 30°C. (**B, C**) Overexpressing the *66–70* mutant partially suppresses its 43S assembly defect. 43S assembly was measured in HCHO crosslinked cells of the strains described in (A) and quantified as described in Figure 2. (**D**) The *66–70* mutation reduces the affinity of eIF1A for 40S subunits *in vitro*. Dissociation of preformed 40S/eIF1A-TAMRA complex in the presence of increasing concentrations of unlabeled WT or mutant eIF1A and 1 μM eIF1 was measured by the decrease in fluorescence anisotropy. (**E**) K_d values (nM) were calculated from the curves in (D) and reported as means ± s.e. (**F**) Rate of TC binding to 40S subunits is reduced by Δ*C in vitro*. Binding of TC to 40S subunits as a function of time (in reactions also containing eIF1, model mRNA and 1 μM WT or mutant eIF1A) was measured as the fraction of [^{35}S]-Met-tRNA$_i^{Met}$ associated with the 40S in a native gel assay. The apparent TC-binding defect in the *66–70* mutant is suppressed by increasing its concentration to 10 μM.

the mutant extract during centrifugation.) Consistent with the partial suppression of the growth defect in *98–101* cells by hc-TC, the 40S-binding defects of eIF2, eIF3 and eIF5, and the mutant eIF1A were diminished by hc-TC in this strain (Figures 6A and B, cf. *98–101*/vector and *98–101*/hc-TC). The fact that eIF3 and eIF5 recruitment was not fully rescued

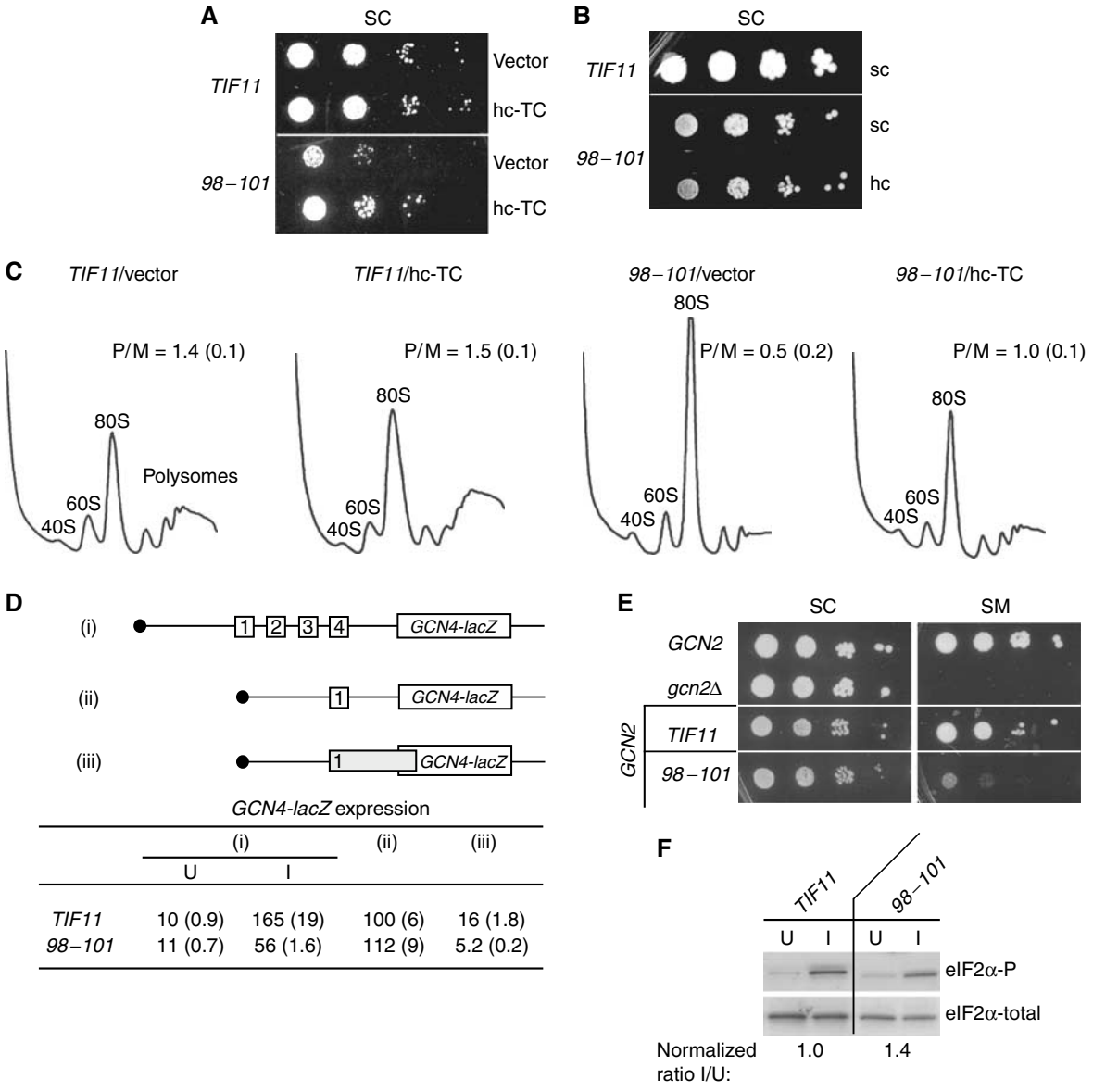

Figure 5 The *98–101* mutation confers a general initiation defect partially suppressed by hc-TC and also a Gcn$^-$ phenotype. (**A**) Serial dilutions of *GCN2* strains H3583 and H3584 transformed with vector YEp24 or hc-TC plasmid p1780-IMT were spotted on SC-U and grown at 30°C for 2 days. (**B**) Serial dilutions of *GCN2* strains containing sc WT *TIF11-FL* (H3583) or *tif11-98–101-FL* on an sc (H3584) or hc (H3585) plasmid were spotted on SC-L and grown at 30°C for 3 days. (**C**) Polysome profiles of the *TIF11* and *98–101* transformants described in (A) were determined as described in Figure 2A. (**D**) The Gcn$^-$ phenotype of the *98–101* allele is not caused by impaired reinitiation or by leaky-scanning of uORF1. The *GCN2* strains H3583 and H3584 harboring plasmids p180, pM199 or pM226, containing *GCN4-lacZ* reporters depicted schematically in (i), (ii) and (iii), respectively, were assayed for β-galactosidase activity after culturing in the absence (U) or presence (I) of 0.5 μg/ml SM for reporter (i), or in the absence of SM for reporters (ii) and (iii). Units of specific activity are means ± s.e. ($n = 6$). (**E**) The *98–101* mutation confers a Gcn$^-$ phenotype. *GCN2* strains H3583 and H3584, together with H1642 harboring YCplac111 and H2999, were spotted on SC-L, and SC lacking Leu, Ile and Val (SC-LIV) + 1 μg/ml SM, and grown at 30°C for 3–4 days. (**F**) The *98–101* mutation does not reduce eIF2α phosphorylation. The *GCN2* strains H3583 and H3584 were grown to $OD_{600} \approx 1$ in SC (U, uninducing) or SC-IV (I, inducing) medium and 0.5 μg/ml SM was added to the latter for 3 h at 30°C. WCEs were subjected to Western analysis using antibodies specific for eIF2α phosphorylated on Ser-51 (eIF2α-P; upper panel) and antibodies against total eIF2α lower panel), and the mean ratios of eIF2α-P/eIF2α were calculated and normalized to the WT ratio in each medium from two independent experiments.

by hc-TC in the *98–101* mutant indicates that this mutation also impairs 40S-binding of these factors by a TC-independent mechanism.

Although *98–101* reduces 40S-binding of eIF1A *in vivo* by ~60% (Figure 6C), analysis of recombinant *98–101* protein *in vitro* revealed no reduction in its intrinsic affinity for the 40S subunit (Figures 4D and E). This suggests that the impaired 40S-binding of the *98–101* protein *in vivo* results from defective interactions with other eIFs that promote PIC assembly, rather than loss of a direct contact between eIF1A and the 40S subunit. This interpretation is supported by the fact that hc-TC increased binding of the *98–101* protein in parallel with that of eIF3 and eIF5 (Figures 6B and C). Overexpression of the *98–101* protein from an hc plasmid fully suppressed its 40S-binding defect, giving 240 ± 70% of WT binding (data not shown), but did not diminish the growth defect (Figure 5B) or 40S-binding defects of eIF2, eIF3 or eIF5 produced by this mutation (increases of <20%

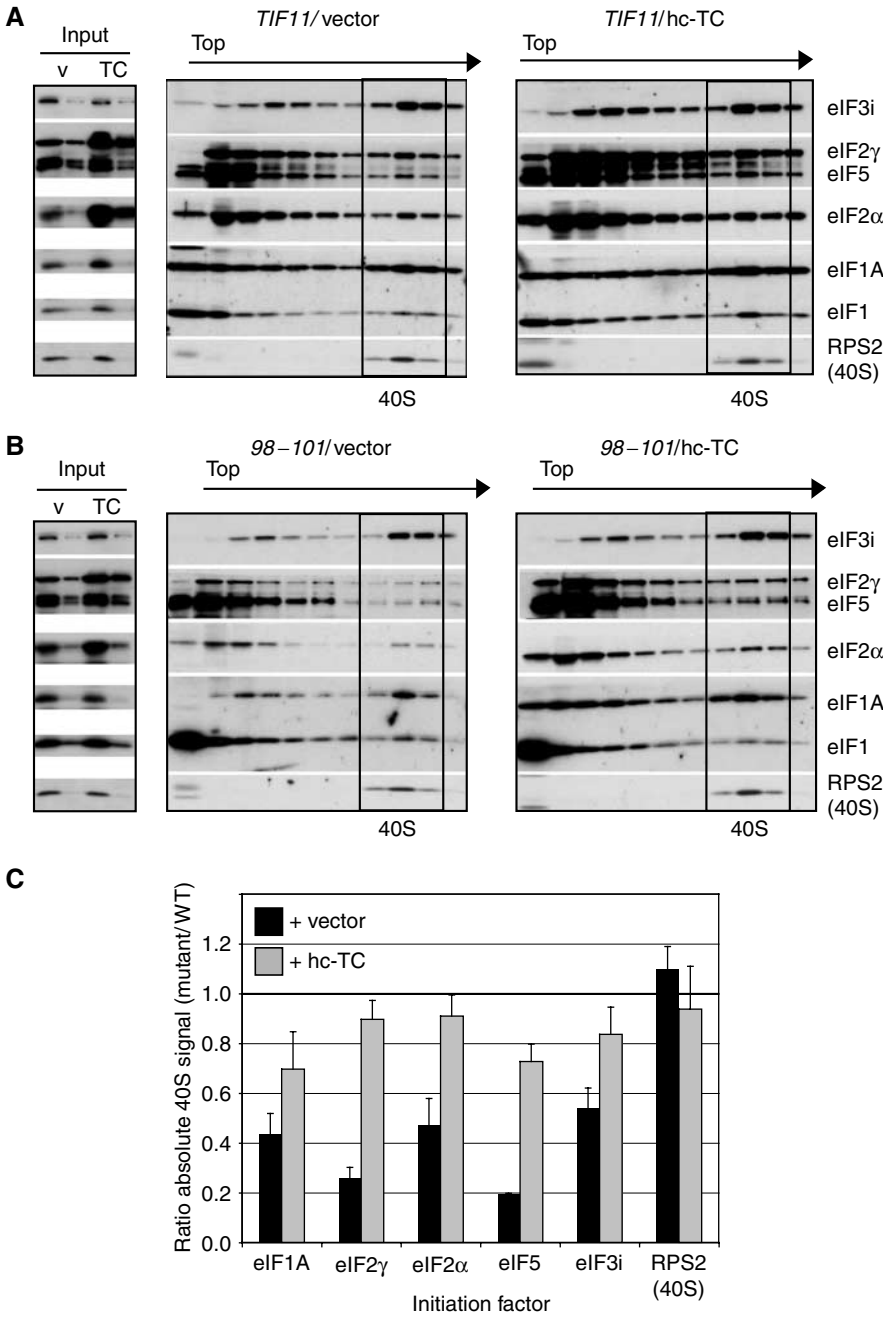

Figure 6 The *98–101* allele confers a defect in 43S assembly that is rescued by TC overexpression. (**A–C**) 43S assembly was measured in HCHO crosslinked cells of strains H3583 and H3584 bearing empty vector or hc-TC plasmid p1780-IMT, as described in Figure 2. The results quantified in panel C are means ± s.e., $n = 3$.

compared to sc *98–101*). Together, our findings suggest that *98–101* impairs a biochemical function of the helical domain required for WT PIC assembly *in vivo* rather than disrupting a critical contact between eIF1A and the ribosome.

The *98–101* mutation increases, rather than decreases, the rate of TC binding to 40S subunits in the reconstituted system containing purified eIF1, TC and mutant eIF1A (Figure 4F). Thus, *98–101* does not disrupt an inherent function of eIF1A in promoting TC recruitment in the manner observed for the Δ*C* mutation. To reconcile this conclusion with our finding that TC recruitment is impaired in *98–101* cells, and that hc-TC suppresses this defect (Figure 6), we suggest that the deficits in eIF5 and eIF3 recruitment produced by *98–101* *in vivo* decrease TC recruitment indirectly because of coupled 40S-binding by these factors in the context of the MFC. Overexpressing TC compensates for these defects in eIF5 and eIF3 recruitment and thereby restores 40S-binding of all three MFC components through mass action and cooperative binding to the 40S subunit.

Evidence that the 98–101 and ΔC mutations produce defects in scanning and AUG selection

Even though the *98–101* mutation reduces TC recruitment *in vivo*, it does not elicit a Gcd$^-$ phenotype (Figure 1B). This suggests that the mutation produces a postassembly defect that suppresses the derepression of *GCN4* translation

expected from impaired TC recruitment. A similar phenomenon has been described for mutations in eIF5 that produce multiple defects in the initiation pathway by disrupting the MFC (Nielsen *et al*, 2004; Singh *et al*, 2005). Supporting this interpretation, *98–101* produces a Gcn$^-$ phenotype in a *GCN2*$^+$ strain, decreasing *GCN4-lacZ* expression to ~30% of WT in response to Ile/Val starvation (Figure 5D, construct i) and conferring sensitivity to an inhibitor of isoleucine/valine biosynthesis (sulfometuron methyl (SM)) (Figure 5E). The Gcn$^-$ phenotype of the *98–101* mutant does not arise from diminished eIF2α phosphorylation in the starved cells (Figure 5F).

One explanation for a Gcn$^-$ phenotype in cells containing ample phosphorylated eIF2α is that ribosomes leaky-scan through the uORF1 AUG and initiate first at uORFs 2, 3 or 4 instead. Following translation of these uORFs, the ribosomes dissociate from the mRNA and fail to reach the *GCN4* start codon. To address this possibility, we assayed a *GCN4-lacZ* reporter containing only an elongated version of uORF1 that overlaps the *GCN4* start codon (Figure 5D, construct iii). Expression of this construct is normally very low because nearly all 40S ribosomes translate uORF1 but fail to reinitiate at *GCN4*, as elongating uORF1 destroys its ability to retain 40S subunits that resume scanning after termination (Grant *et al*, 1994). Leaky-scanning of the elongated uORF1 in response to the *98–101* mutation would be expected to increase expression of this reporter; however, we observed decreased reporter expression instead (~30% of WT; Figure 5D, iii). Thus, *98–101* leads to lower, rather than higher, leaky-scanning through uORF1.

Another possible explanation for the Gcn$^-$ phenotype of *98–101* is that it impairs the ability of 40S subunits to resume scanning and reinitiate at *GCN4* following translation of uORF1. This mechanism can also be eliminated because *98–101* does not decrease expression of the *GCN4-lacZ* reporter containing only WT uORF1 (Figure 5D, construct ii). This last finding, that eliminating uORFs 2–4 suppresses the deleterious effect of *98–101* on *GCN4* translation, strongly suggests that the Gcn$^-$ phenotype results from the inability of rescanning 40S subunits to bypass uORFs 2–4 even when TC recruitment is diminished by eIF2α phosphorylation. A Gcn$^-$ phenotype with the same characteristics was observed previously when the distance between uORFs 1 and 4 was expanded to provide increased time for rebinding of TC before the rescanning 40S subunits reach uORF4 (Abastado *et al*, 1991). Hence, *98–101* may mimic the effect of increased uORF1–4 separation by reducing the rate of 40S scanning between uORFs 1 and 4. A reduced efficiency of scanning could also explain the decrease in leaky-scanning past elongated uORF1 produced by *98–101* (Figure 5D, iii), as a structural impediment to scanning was shown previously to reduce leaky-scanning through an AUG codon (Kozak, 1990).

We sought next to obtain biochemical evidence that the *98–101* mutation decreases the efficiency of ribosomal scanning. Mammalian eIF1A participates with eIF1 in allowing the 43S complex to scan from the 5′-end of mRNA and form a stable 48S complex at the start codon in reactions containing purified ribosomes, eIFs and β-globin mRNA. Inhibition of primer extension by reverse transcriptase is used to map the leading edge of the ribosome in the 48S complexes (toe-printing) (Pestova *et al*, 1998). We first demonstrated that yeast eIF1A can substitute for mammalian eIF1A in such reactions, and then examined the effects of eIF1A mutations on this activity.

With all human factors except eIF1A present, a significant proportion of 48S complexes were formed with the AUG codon in the P-site, yielding toe-prints 16 nucleotides (nt) downstream of the start codon (complex II) (Figure 7A). A sizable fraction of aberrant complexes also occurred with toe-prints 16 nt from a near-cognate GUG codon. Smaller proportions of aberrant complexes near the 5′-terminus (complex I) or with toe-prints 7 nt upstream of complex II (designated complex III) also formed in the absence of eIF1A. Supplementation with WT yeast or human eIF1A eliminated or strongly suppressed formation of complex I and the GUG complex, while yeast eIF1A also suppressed complex III (Figure 7A). Thus, WT yeast eIF1A functions efficiently in this assay to promote nearly exclusive formation of 48S PICs at the AUG codon.

Interestingly, the *98–101* and Δ*C* proteins allowed formation of complex I and the GUG complex at levels ~50% of that observed in the absence of eIF1A, whereas a different yeast mutant (*GRRGK*$_{12-16}$*AAAAA*) showed WT inhibition of these aberrant complexes. The latter finding is significant because the *GRRGK*$_{12-16}$*AAAAA* mutant showed a lower affinity for 40S ribosomes in the binding assays of Figures 4D and E than did the *98–101* mutant (data not shown). Hence, it is unlikely that the mutant phenotypes of *98–101* (or Δ*C*) in the toe-print assays arise from reduced 40S-binding of mutant eIF1A proteins. We interpret these results to indicate that *98–101*, and Δ*C* decrease the propensity of the 43S complex to scan the mRNA, increasing the stability of aberrant 48S complexes upstream of the AUG start codon (Battiste *et al*, 2000).

Finally, we asked whether the *98–101* or Δ*C* mutations lead to increased utilization of a near-cognate start codon *in vivo*. This defect can be detected by increased initiation at a UUG triplet in the 5′-end of the *HIS4* ORF, allowing expression of the *his4-303* allele lacking the normal AUG start codon. The resulting histidine auxotrophy indicates a Sui$^-$ (suppressor of initiation codon mutation) phenotype (Donahue, 2000). The Δ*C* mutation strongly suppressed the His$^-$ phenotype of *his4-303*, conferring a robust Sui$^-$ phenotype (Figure 7C). Furthermore, we found that Δ*C* is lethal in the presence of a dominant Sui$^-$ allele of *TIF5* encoding a hyperactive form of eIF5 that likely produces a Sui$^-$ phenotype by increasing GTP hydrolysis at UUG codons (Huang *et al*, 1997). The synthetic lethality of the *SUI5 tif11-*Δ*C* combination may result from an intolerable level of initiation at near-cognate start codons. Although the *98–101* mutation did not suppress the His$^-$ phenotype associated with *his4-303* (data not shown), it produced a 2.4-fold increase in translation of a *his4-lacZ* reporter containing UUG versus AUG as the start codon (Figure 7B). Hence, we believe that *98–101* also confers a Sui$^-$ phenotype, but weaker than that of Δ*C*.

Discussion

Our finding that the Δ*C* and *66–70* mutations derepress *GCN4* translation in a manner suppressed by TC overexpression provides genetic evidence that eIF1A promotes TC recruitment *in vivo*. Consistent with this, we showed that both mutations impair binding of TC, eIF3 and eIF5 to 40S subunits *in vivo*, and that the defects in TC recruitment can be

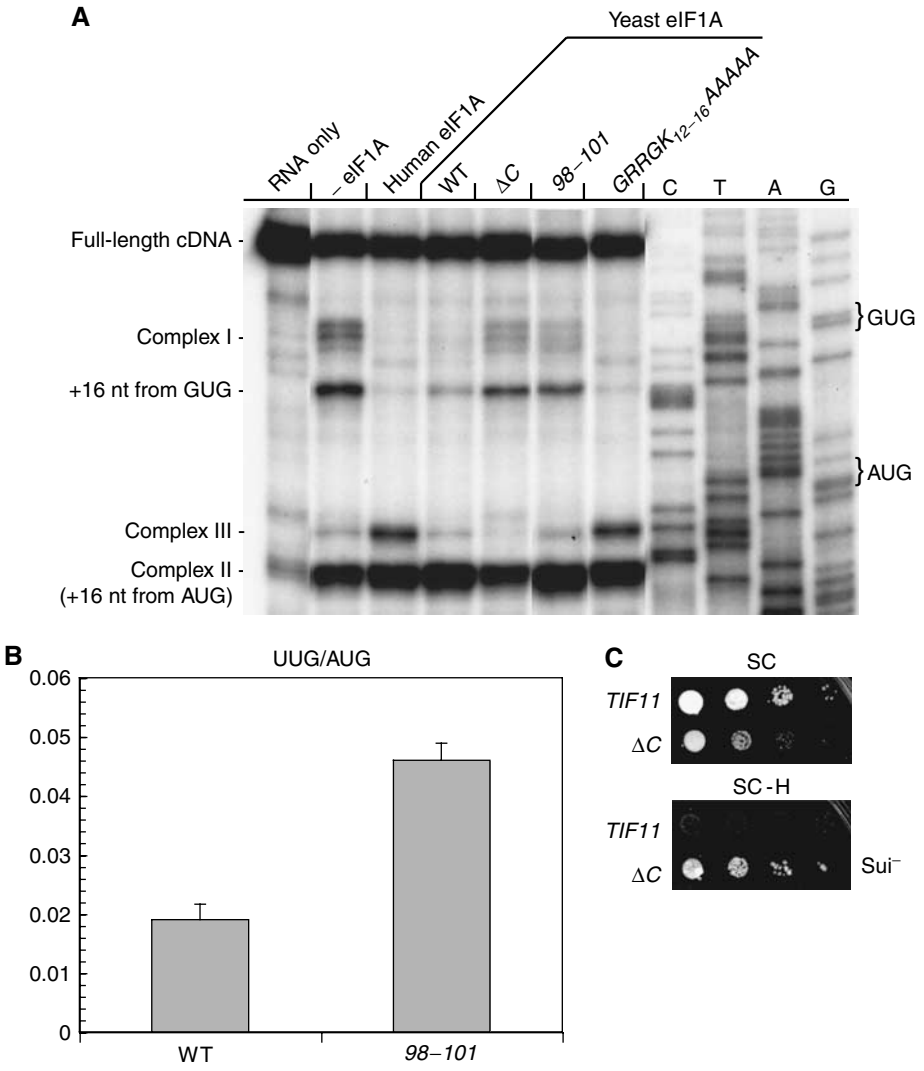

Figure 7 C-terminal mutations in eIF1A cause scanning/AUG recognition defects *in vitro* and *in vivo*. (**A**) Toe-printing analysis of 48S complexes on β-globin mRNA in reaction mixtures containing 40S subunits and mammalian translation initiation factors in the absence or presence of eIF1A, as indicated. See text for explanation of different complexes labeled on the left. (**B**) The *98–101* mutation increases utilization of a UUG start codon *in vivo*. Strains H3583 and H3584 carrying plasmids YCp50-HIS4-AUG-lacZ or YCp50-HIS4-UUG-lacZ were grown in SC-U medium and assayed for β-galactosidase activity. The specific activities ± s.e. ($n = 6$) determined for the YCp50-HIS4-UUG-lacZ versus YCp50-HIS4-AUG-lacZ transformants were measured in three independent experiments and used to calculate the mean ratios ± s.e. ($n = 3$) shown in the histogram. (**C**) The Δ*C* mutation suppresses the His$^-$ phenotype conferred by the *his4-303* allele. Serial 10-fold dilutions of strains H3583 and H3586 were spotted on SC lacking leucine and histidine and grown at 30°C for 2 days (SC, upper panel) or 14 days (SC-H, lower panel).

overcome through mass action by overexpressing the TC. Both mutations also conferred reduced rates of TC binding to 40S subunits in a reconstituted *in vitro* assay, although the defect produced by *66–70* was suppressed by using elevated levels of the mutant protein to compensate for its defect in 40S-binding. In agreement with this last result, the Slg$^-$ and Gcd$^-$ phenotypes and defects in PIC assembly produced by *66–70 in vivo* were diminished by overexpressing the mutant protein. Thus, the TC recruitment defect and attendant derepression of *GCN4* conferred by *66–70* arise largely from its defect in 40S-binding. This conclusion fits with the prediction from the 30S–IF1 complex (Carter *et al*, 2001) that residues 66–70 in the OB-fold of eIF1A are close to the A-site of the 40S subunit. The Δ*C* mutation, by contrast, impairs 43S assembly even though the mutant eIF1A is bound to 40S subunits at WT or greater levels. Hence, the C-terminal extension or adjacent 3_{10} helix eliminated by Δ*C* appears to have an important biochemical function in TC recruitment.

Whereas overexpressing TC reduced the Gcd$^-$ phenotypes and TC recruitment defects in the *66–70* and Δ*C* mutants, it did not suppress their Slg$^-$ phenotypes nor restore 40S-binding of eIF5 or eIF3 (in the Δ*C* mutant) to WT levels. By contrast, overexpressing eIF5 rescued 40S-binding of eIF5 and diminished the growth defect in *66–70* cells. These results indicate that eIF1A promotes 40S-binding of eIF5 and eIF3 independent of its role in TC recruitment. Hence, we conclude that eIF1A independently promotes the 40S-binding of multiple constituents of the yeast MFC. As no direct physical interactions between eIF1A and MFC components have been described, the molecular basis for the stimulatory effects of eIF1A on MFC recruitment remains to be defined.

The *98–101* substitution in the α-helical domain was the only mutation that conferred a growth defect suppressible by hc-TC, and the mutation also impaired 40S-binding binding of TC, eIF3 and eIF5 *in vivo* in a manner largely corrected by overexpressing TC. The *98–101* mutation impairs 40S-binding of eIF1A itself *in vivo*, and while this defect was corrected by overexpressing the mutant protein, the Slg$^-$ phenotype and reductions in PIC assembly were not simultaneously suppressed. Hence, we conclude that the helical domain of eIF1A has an important function in promoting recruitment of the MFC to the 40S subunit.

The recombinant *98–101* protein exhibits WT affinity for 40S ribosomes *in vitro*, indicating that reduced 40S-binding by this mutant *in vivo* does not reflect loss of a contact between eIF1A and the ribosome. Similarly, *98–101* did not reduce the rate of TC binding to 40S subunits in the reconstituted assay, suggesting that the intrinsic function of eIF1A in TC recruitment is not impaired by this mutation. To reconcile these *in vitro* and *in vivo* findings, we suggest that *98–101* indirectly impairs TC recruitment *in vivo* by reducing 40S-binding of eIF3 and eIF5, thereby disrupting the coupled association of factors in the MFC with the ribosome. We further suggest that 40S-binding of eIF1A is coupled to that of the MFC, so that the *98–101* mutation indirectly impairs 40S-binding of eIF1A by diminishing recruitment of MFC components. Indeed, we recently obtained evidence that depleting eIF5 from cells impairs eIF1A recruitment *in vivo* (A Jivotovskaya, K Nielsen and AGH, unpublished observations). We suggest that overexpressing TC most likely restores 40S-binding of the MFC in the *98–101* mutant by driving the assembly of a TC–eIF5 binary complex on the ribosome by mass action. This in turn would stimulate recruitment of eIF3, as interaction with eIF2 increases the affinity of eIF5 for eIF3 (Singh *et al*, 2004).

Apart from its role in PIC assembly, we found that the C-terminal domain of eIF1A also functions in scanning and AUG recognition. Toe-print analysis of 48S assembly in a reconstituted mammalian system revealed that both the *98–101* and Δ*C* mutations increase formation of aberrant complex I and the 48S complexes at an upstream GUG on β-globin mRNA. As suggested previously (Battiste *et al*, 2000), formation of these aberrant complexes could result from a decreased rate of ribosomal scanning. Consistent with these findings, the *98–101* and Δ*C* mutations appeared to increase utilization of non-AUG triplets as start codons on *HIS4* mRNA *in vivo* (Sui$^-$ phenotype).

A slower rate of scanning can also explain why the defect in TC recruitment conferred by *98–101 in vivo* does not produce a Gcd$^-$ phenotype. In fact, this mutant displays a Gcn$^-$ phenotype in *GCN2* cells that can be attributed to the failure of 40S ribosomes rescanning downstream from uORF1 to bypass uORFs 2–4 even though TC levels are reduced by eIF2α phosphorylation. This type of Gcn$^-$ defect was observed previously when the distance between uORFs 1 and 4 was expanded, increasing the time required for scanning 40S subunits to reach uORF4 after terminating at uORF1. This alteration compensates for the delay in TC binding elicited by eIF2α phosphorylation and ensures that nearly all 40S subunits rebind TC before reaching uORF4 and, hence, fail to reinitiate at *GCN4* (Abastado *et al*, 1991). Thus, we suggest that the *98–101* mutation mimics the effect of lengthening the uORF1–4 interval and produces a Gcn$^-$ phenotype by decreasing the rate of scanning.

It might be expected that the Δ*C* mutation would also confer a Gcn$^-$ phenotype, given that it produced a scanning defect in the toe-print assay comparable to that of *98–101*. In fact, we found that Δ*C* does confer sensitivity to SM and a modest (20%) reduction in *GCN4-lacZ* expression in a *GCN2*$^+$ strain under starvation conditions, without lowering eIF2α phosphorylation (data not shown). Perhaps the defect in TC binding produced by Δ*C* outweighs the scanning defect and suppresses the expected Gcn$^-$ phenotype. In *98–101* cells, by contrast, the scanning defect would outweigh the deficit in TC binding and suppress the expected Gcd$^-$ phenotype.

Support for this interpretation came recently from the analysis of mutations in the eIF5-CTD that destabilize the MFC and produce Gcd$^-$ phenotypes at 30°C but Gcn$^-$ phenotypes at a higher temperature (36°C) where the mutations have a stronger effect on initiation. It was proposed that

Table I Plasmids used in this study

Plasmid	Description	Source or reference
YCplac111	sc *LEU2* cloning vector	Gietz and Sugino (1988)
YEplac181	hc *LEU2* cloning vector	Gietz and Sugino (1988)
p3392	sc *URA3 TIF11* in YCplac33	Olsen *et al* (2003)
p3499	sc *LEU2 TIF11-FL* in YCplac111	Olsen *et al* (2003)
p3604	hc *LEU2 tif11-Δ108–153-FL* in YEplac181	Olsen *et al* (2003)
p4399	sc *LEU2 tif11-RKKVW$_{66–70}$AAAVA-FL* in YCplac111	This study
p4443	hc *LEU2 tif11-RKKVW$_{66–70}$AAAVA-FL* in YEplac181	This study
p4398	sc *LEU2 tif11-DEAR$_{98–101}$AAAA-FL* in YCplac111	This study
p4444	hc *LEU2 tif11-DEAR$_{98–101}$AAAA-FL* in YEplac181	This study
p1780-IMT	hc *URA3 SUI2*, *GCD11*, *SUI3*, *IMT4* in YEp24	Asano *et al* (1999)
YEp24	hc *URA3* cloning vector	Parent *et al* (1985)
YEpTIF5-U	hc *URA3 TIF5-FL* in YEplac195	Valasek *et al* (2004)
YEplac195	hc *URA3*	Gietz and Sugino (1988)
p4385	hc *TRP1 SUI2*, *GCD11*, *SUI3*, *IMT4* in YEp24, *ura3*::*TRP1:kan^R*	This study
YEplac112	hc *TRP1*	Gietz and Sugino (1988)
p180	sc *URA3 GCN4-lacZ* with WT leader	Hinnebusch (1985)
PM199	sc *URA3 GCN4-lacZ* with uORF1 only	Grant *et al* (1994)
PM226	sc *URA3 GCN4-lacZ* with uORF1 extending into *GCN4*	Grant *et al* (1994)
p367	sc *URA3 AUG-HIS4-lacZ*	Donahue and Cigan (1988)
p391	sc *URA3 AUU-HIS4-lacZ*	Donahue and Cigan (1988)

Table II Yeast strains used in this study

Strain	Genotype	Source
H1642	*MATa ura3–52 leu2–3 leu2–112 trp1Δ63* <*GCN4-lacZ, TRP1*>	Dever *et al* (1992)
H2809	*MATa ura3–52 leu2–3 leu2–112 trp1Δ63 gcn2Δ tif11Δ* <*GCN4-lacZ, TRP1*>*p3392* (*sc TIF11, URA3*)	Choi *et al* (2000)
H2999	*MATa ura3–52 leu2–3 leu2–112 trp1Δ63 gcn2Δ tif11Δ* <*GCN4-lacZ, TRP1*>*p3499* (*sc TIF11-FL, LEU2*)	Olsen *et al* (2003)
H3002	*MATa ura3–52 leu2–3 leu2–112 trp1Δ63 gcn2Δ tif11Δ* <*GCN4-lacZ, TRP1*>*p3604* (*hc tif11-Δ108–153-FL, LEU2*)	Olsen *et al* (2003)
H3580	*MATa ura3–52 leu2–3 leu2–112 trp1Δ63 gcn2Δ tif11Δ* <*GCN4-lacZ, TRP1*>*p4399* (*sc tif11-RKKVW*$_{66–70}$*AAAVA-FL, LEU2*)	This study
H3581	*MATa ura3–52 leu2–3 leu2–112 trp1Δ63 gcn2Δ tif11Δ* <*GCN4-lacZ, TRP1*>*p4443* (*hc tif11-RKKVW*$_{66–70}$*AAAVA-FL, LEU2*)	This study
H3582	*MATa ura3–52 trp1Δ63 leu2–3, leu2–112 his4–303* (*ATT*) *tif11Δ p3392* (*sc TIF11, URA3*)	This study
H3583	*MATa ura3–52 trp1Δ63 leu2–3, leu2–112 his4–303* (*ATT*) *tif11Δp3499* (*sc TIF11-FL, LEU2*)	This study
H3584	*MATa ura3–52 trp1Δ63 leu2–3, leu2–112 his4–303* (*ATT*) *tif11Δp4398* (*sc tif11-DEAR*$_{98–101}$*AAAA-FL, LEU2*)	This study
H3585	*MATa ura3–52 trp1Δ63 leu2–3, leu2–112 his4–303* (*ATT*) *tif11Δ p4444* (*hc tif11-DEAR*$_{98–101}$*AAAA-FL, LEU2*)	This study
H3586	*MATa ura3–52 trp1Δ63 leu2–3, leu2–112 his4–303* (*ATT*) *tif11Δ p3604* (*hc tif11-Δ108–153-FL, LEU2*)	This study

impaired TC recruitment at 30°C produces the Gcd$^-$ phenotype but more severe disruption of the MFC at 36°C elicits a scanning defect (leaky-scanning of uORF1 in this case) that outweighs the effect of reduced TC recruitment on *GCN4* translation (Singh *et al*, 2005). We suggest that the Δ*C* and *98–101* mutations can be likened to these eIF5-CTD mutations at 30 and 36°C, respectively, in terms of their relative effects on TC recruitment versus scanning. Singh *et al* (2005) also showed that certain eIF5-CTD mutants display a Gcd$^-$ phenotype only when eIF1 is overexpressed, apparently because eIF1 overexpression exacerbates a moderate defect in TC recruitment to the point where it outweighs the scanning defects produced by these eIF5 mutations, thus derepressing *GCN4*. Consistent with this, we found that eIF1 overexpression reveals a Gcd$^-$ phenotype in the *98–101* mutant and exacerbates the Gcd$^-$ phenotype of Δ*C* (data not shown).

Our results show that the α-helical domain and random-coil CTD of eIF1A, regions not present in bacterial IF1, stimulate binding of TC and other MFC components to the 40S subunit and promote efficient scanning and AUG selection. Residues 66–70 in the OB-fold, by contrast, likely provide a critical 40S–eIF1A interaction. It makes sense that functions of eIF1A involved in MFC recruitment and scanning depend on domains not present in IF1, as eIF2, eIF3 and eIF5 are absent in bacteria, and there are significant differences in Met-tRNA$_i^{Met}$ recruitment and start codon recognition between eukaryotes and prokaryotes.

Materials and methods

Yeast strains and plasmid construction

The plasmids and yeast strains involving the *66–70*, *98–101* and Δ*C* mutations are listed in Tables I and II. All other plasmids and yeast strains for the remaining *TIF11* mutations are listed in the Supplementary data along with details of their construction, and the biochemical and genetic methods employed.

Supplementary data

Supplementary data are available at *The EMBO Journal* Online.

Acknowledgements

We thank Tom Dever and members of our laboratories for helpful suggestions.

References

Abastado JP, Miller PF, Jackson BM, Hinnebusch AG (1991) Suppression of ribosomal reinitiation at upstream open reading frames in amino acid-starved cells forms the basis for *GCN4* translational control. *Mol Cell Biol* **11:** 486–496

Algire MA, Maag D, Savio P, Acker MG, Tarun Jr SZ, Sachs AB, Asano K, Nielsen KH, Olsen DS, Phan L, Hinnebusch AG, Lorsch JR (2002) Development and characterization of a reconstituted yeast translation initiation system. *RNA* **8:** 382–397

Asano K, Clayton J, Shalev A, Hinnebusch AG (2000) A multifactor complex of eukaryotic initiation factors eIF1, eIF2, eIF3, eIF5, and initiator tRNA^{Met} is an important translation initiation intermediate *in vivo*. *Genes Dev* **14:** 2534–2546

Asano K, Krishnamoorthy T, Phan L, Pavitt GD, Hinnebusch AG (1999) Conserved bipartite motifs in yeast eIF5 and eIF2Bε, GTPase-activating and GDP-GTP exchange factors in translation initiation, mediate binding to their common substrate eIF2. *EMBO J* **18:** 1673–1688

Asano K, Shalev A, Phan L, Nielsen K, Clayton J, Valášek L, Donahue TF, Hinnebusch AG (2001) Multiple roles for the carboxyl terminal domain of eIF5 in translation initiation complex assembly and GTPase activation. *EMBO J* **20:** 2326–2337

Battiste JB, Pestova TV, Hellen CUT, Wagner G (2000) The eIF1A solution structure reveals a large RNA-binding surface important for scanning function. *Mol Cell* **5:** 109–119

Carter AP, Clemons Jr WM, Brodersen DE, Morgan-Warren RJ, Hartsch T, Wimberly BT, Ramakrishnan V (2001) Crystal structure of an initiation factor bound to the 30S ribosomal subunit. *Science* **291:** 498–501

Choi SK, Olsen DS, Roll-Mecak A, Martung A, Remo KL, Burley SK, Hinnebusch AG, Dever TE (2000) Physical and functional interaction between the eukaryotic orthologs of prokaryotic translation initiation factors IF1 and IF2. *Mol Cell Biol* **20:** 7183–7191

Cross FR (1997) 'Marker swap' plasmids: convenient tools for budding yeast molecular genetics. *Yeast* **13:** 647–653

DeLano WL (2002) *The PyMOL Molecular Graphics System*. San Carlos, CA: DeLano Scientific. http://www.pymol.org

Dever TE, Feng L, Wek RC, Cigan AM, Donahue TD, Hinnebusch AG (1992) Phosphorylation of initiation factor 2α by protein kinase GCN2 mediates gene-specific translational control of *GCN4* in yeast. *Cell* **68:** 585–596

Dever TE, Yang W, Åström S, Byström AS, Hinnebusch AG (1995) Modulation of $tRNA_i^{Met}$, eIF-2 and eIF-2B expression shows that *GCN4* translation is inversely coupled to the level of eIF-2.GTP.Met-$tRNA_i^{Met}$ ternary complexes. *Mol Cell Biol* **15:** 6351–6363

Donahue T (2000) Genetic approaches to translation initiation in *Saccharomyces cerevisiae*. In *Translational Control of Gene Expression*, Sonenberg N, Hershey JWB and Mathews MB (eds), pp 487–502. Cold Spring Harbor, NY: Cold Spring Harbor Laboratory Press

Donahue TF, Cigan AM (1988) Genetic selection for mutations that reduce or abolish ribosomal recognition of the *HIS4* translational initiator region. *Mol Cell Biol* **8:** 2955–2963

Gietz RD, Sugino A (1988) New yeast—*Escherichia coli* shuttle vectors constructed with *in vitro* mutagenized yeast genes lacking six-base pair restriction sites. *Gene* **74:** 527–534

Grant CM, Miller PF, Hinnebusch AG (1994) Requirements for intercistronic distance and level of eIF-2 activity in reinitiation on *GCN4* mRNA varies with the downstream cistron. *Mol Cell Biol* **14:** 2616–2628

Guex N, Peitsch MC (1997) SWISS-MODEL and the Swiss-PdbViewer: an environment for comparative protein modeling. *Electrophoresis* **18:** 2714–2723

He H, von der Haar T, Singh CR, Ii M, Li B, Hinnebusch AG, McCarthy JE, Asano K (2003) The yeast eukaryotic initiation factor 4G (eIF4G) HEAT domain interacts with eIF1 and eIF5 and is involved in stringent AUG selection. *Mol Cell Biol* **23:** 5431–5445

Hershey JWB, Merrick WC (2000) Pathway and mechanism of initiation of protein synthesis. In *Translational Control of Gene Expression*, Sonenberg N, Hershey JWB and Mathews MB (eds), pp 33–88. Cold Spring Harbor, NY: Cold Spring Harbor Laboratory Press

Hinnebusch AG (1985) A hierarchy of *trans*-acting factors modulate translation of an activator of amino acid biosynthetic genes in *Saccharomyces cerevisiae*. *Mol Cell Biol* **5:** 2349–2360

Hinnebusch AG (1996) Translational control of *GCN4*: gene-specific regulation by phosphorylation of eIF2. In *Translational Control*, Hershey JWB, Mathews MB and Sonenberg N (eds), pp 199–244. Cold Spring Harbor, NY: Cold Spring Harbor Laboratory Press

Hinnebusch AG (2000) Mechanism and regulation of initiator methionyl-tRNA binding to ribosomes. In *Translational Control of Gene Expression*, Sonenberg N, Hershey JWB and Mathews MB (eds), pp 185–243. Cold Spring Harbor, NY: Cold Spring Harbor Laboratory Press

Huang H, Yoon H, Hannig EM, Donahue TF (1997) GTP hydrolysis controls stringent selection of the AUG start codon during translation initiation in *Saccharomyces cerevisiae*. *Genes Dev* **11:** 2396–2413

Kolupaeva VG, Unbehaun A, Lomakin IB, Hellen CU, Pestova TV (2005) Binding of eukaryotic initiation factor 3 to ribosomal 40S subunits and its role in ribosomal dissociation and anti-association. *RNA* **11:** 470–486

Kozak M (1990) Downstream secondary structure facilitates recognition of initiator codons by eukaryotic ribosomes. *Proc Natl Acad Sci USA* **87:** 8301–8305

Maag D, Fekete CA, Gryczynski Z, Lorsch JR (2005) A conformational change in the eukaryotic translation preinitiation complex and release of eIF1 signal recognition of the start codon. *Mol Cell* **17:** 265–275

Maag D, Lorsch JR (2003) Communication between eukaryotic translation initiation factors 1 and 1A on the yeast small ribosomal subunit. *J Mol Biol* **330:** 917–924

Majumdar R, Bandyopadhyay A, Maitra U (2003) Mammalian translation initiation factor eIF1 functions with eIF1A and eIF3 in the formation of a stable 40S preinitiation complex. *J Biol Chem* **278:** 6580–6587

Moazed D, Samaha RR, Gualerzi C, Noller HF (1995) Specific protection of 16S rRNA by translational initiation factors. *J Mol Biol* **248:** 207–210

Moehle CM, Hinnebusch AG (1991) Association of RAP1 binding sites with stringent control of ribosomal protein gene transcription in *Saccharomyces cerevisiae*. *Mol Cell Biol* **11:** 2723–2735

Nielsen KH, Szamecz B, Valasek L, Jivotovskaya A, Shin BS, Hinnebusch AG (2004) Functions of eIF3 downstream of 48S assembly impact AUG recognition and *GCN4* translational control. *EMBO J* **23:** 1166–1177

Olsen DS, Savner EM, Mathew A, Zhang F, Krishnamoorthy T, Phan L, Hinnebusch AG (2003) Domains of eIF1A that mediate binding to eIF2, eIF3 and eIF5B and promote ternary complex recruitment *in vivo*. *EMBO J* **22:** 193–204

Parent SA, Fenimore CM, Bostian KA (1985) Vector systems for the expression, analysis and cloning of DNA sequences in *S.cerevisiae*. *Yeast* **1:** 83–138

Pestova TV, Borukhov SI, Hellen CUT (1998) Eukaryotic ribosomes require initiation factors 1 and 1A to locate initiation codons. *Nature* **394:** 854–859

Pestova TV, Kolupaeva VG (2002) The roles of individual eukaryotic translation initiation factors in ribosomal scanning and initiation codon selection. *Genes Dev* **16:** 2906–2922

Phan L, Zhang X, Asano K, Anderson J, Vornlocher HP, Greenberg JR, Qin J, Hinnebusch AG (1998) Identification of a translation initiation factor 3 (eIF3) core complex, conserved in yeast and mammals, that interacts with eIF5. *Mol Cell Biol* **18:** 4935–4946

Sette M, van Tilborg P, Spurio R, Kaptein R, Paci M, Gualerzi CO, Boelens R (1997) The structure of the translational initiation factor IF1 from *E. coli* contains an oligomer-binding motif. *EMBO J* **16:** 1436–1443

Sherman F, Fink GR, Lawrence CW (1974) *Methods of Yeast Genetics*, pp 61–64. Cold Spring Harbor, NY: Cold Spring Harbor Laboratory Press

Singh CR, Curtis C, Yamamoto Y, Hall NS, Kruse DS, He H, Hannig EM, Asano K (2005) Eukaryotic translation initiation factor 5 is critical for integrity of the scanning preinitiation complex and accurate control of *GCN4* translation. *Mol Cell Biol* **25:** 5480–5491

Singh CR, Yamamoto Y, Asano K (2004) Physical association of eukaryotic initiation factor (eIF) 5 carboxyl-terminal domain with the lysine-rich eIF2beta segment strongly enhances its binding to eIF3. *J Biol Chem* **279:** 49644–49655

Thompson JD, Higgins DG, Gibson TJ (1994) CLUSTAL W: improving the sensitivity of progressive multiple sequence alignment through sequence weighting, positions-specific gap penalties and weight matrix choice. *Nucleic Acids Res* **22:** 4673–4680

Valášek L, Mathew A, Shin BS, Nielsen KH, Szamecz B, Hinnebusch AG (2003) The yeast eIF3 subunits TIF32/a and NIP1/c and eIF5 make critical connections with the 40S ribosome *in vivo*. *Genes Dev* **17:** 786–799

Valášek L, Nielsen KH, Hinnebusch AG (2002) Direct eIF2–eIF3 contact in the multifactor complex is important for translation initiation *in vivo*. *EMBO J* **21:** 5886–5898

Valasek L, Nielsen KH, Zhang F, Fekete CA, Hinnebusch AG (2004) Interactions of eukaryotic translation initiation factor 3 (eIF3) subunit NIP1/c with eIF1 and eIF5 promote preinitiation complex assembly and regulate start codon selection. *Mol Cell Biol* **24:** 9437–9455